Heparan Sulfate Proteoglycans Provide a Signal to *Plasmodium* Sporozoites to Stop Migrating and Productively Invade Host Cells

Alida Coppi,[1] Rita Tewari,[2] Joseph R. Bishop,[3] Brandy L. Bennett,[1] Roger Lawrence,[3] Jeffrey D. Esko,[3] Oliver Billker,[2] and Photini Sinnis[1,*]

[1]Department of Medical Parasitology, 341 East 25th Street, New York University School of Medicine, New York, NY 10010, USA
[2]Division of Cell and Molecular Biology, Imperial College London, London SW7 2AZ, UK
[3]Department of Cellular and Molecular Medicine, University of California, San Diego, 9500 Gilman Drive, La Jolla, CA 92093, USA
*Correspondence: photini.sinnis@nyu.edu
DOI 10.1016/j.chom.2007.10.002

SUMMARY

Malaria infection is initiated when *Anopheles* mosquitoes inject *Plasmodium* sporozoites into the skin. Sporozoites subsequently reach the liver, invading and developing within hepatocytes. Sporozoites contact and traverse many cell types as they migrate from skin to liver; however, the mechanism by which they switch from a migratory mode to an invasive mode is unclear. Here, we show that sporozoites of the rodent malaria parasite *Plasmodium berghei* use the sulfation level of host heparan sulfate proteoglycans (HSPGs) to navigate within the mammalian host. Sporozoites migrate through cells expressing low-sulfated HSPGs, such as those in skin and endothelium, while highly sulfated HSPGs of hepatocytes activate sporozoites for invasion. A calcium-dependent protein kinase is critical for the switch to an invasive phenotype, a process accompanied by proteolytic cleavage of the sporozoite's major surface protein. These findings explain how sporozoites retain their infectivity for an organ that is far from their site of entry.

INTRODUCTION

Infection of the mammalian host with malaria is initiated when *Plasmodium* sporozoites are injected into the skin as the mosquito probes for blood (reviewed in Sinnis and Coppi, 2007). Live imaging studies show that a proportion of the injected sporozoites actively move within the dermis in a random fashion and eventually contact blood vessels which they penetrate to enter the blood circulation (Amino et al., 2006). Once in the circulation, sporozoites arrest in the liver, cross the sinusoidal barrier and invade hepatocytes where they develop into exoerythrocytic forms (EEFs).

Sporozoites must traverse several cell barriers as they make their way from the skin to the liver. Previous studies have shown that sporozoites can interact with cells in one of two ways: they can productively invade a cell, forming a parasitophorous vacuole in which they will replicate, or they can migrate through a cell, breaching the cell's plasma membrane in the process (Mota et al., 2001). The ability to traverse cell barriers likely enables sporozoites to reach the liver from their injection site in the dermis. Indeed mutants lacking this ability have reduced infectivity in vivo but not in vitro when they are placed directly on hepatocytes (Bhanot et al., 2005; Ishino et al., 2004).

The molecular signals that allow sporozoites to know where they are and "decide" whether to continue to migrate or prepare for cell invasion are not known. That the sporozoite recognizes different cell types was suggested by recent studies on the proteolytic cleavage of the sporozoite's major surface protein, the circumsporozoite protein (CSP; Coppi et al., 2005). CSP is processed by a parasite cysteine protease and cleavage is specifically associated with productive invasion and not cell traversal. Since sporozoites contact cells during both invasion of and migration through cells, these data suggested that sporozoites recognize different cell surface molecule(s) on permissive versus non-permissive cells. Sporozoites are known to bind heparan sulfate proteoglycans (HSPGs; reviewed in Sinnis and Coppi, 2007). Using the rodent malaria model, *Plasmodium berghei*, we show that contact with cells expressing highly sulfated HSPGs activate sporozoites to begin the invasion process. In contrast, contact with less sulfated HSPGs results in continued migration through cells. Furthermore, we show that the transition from a migratory to an invasive phenotype is mediated by a signaling pathway that includes a new member of a family of calcium-dependent protein kinases.

RESULTS

A New Sporozoite Migration Assay

We began by developing a quantitative migration assay since the currently used assay, in which fluorescently labeled dextran is taken up by cells that are wounded during sporozoite migration, allows one to observe wounded cells but does not quantify the frequency with which a cell is wounded (Mota et al., 2001). When added to cell
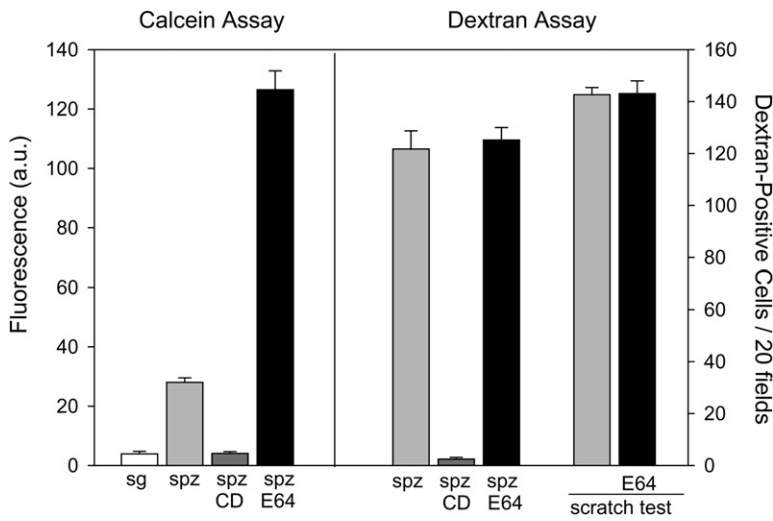
Figure 1. A New Sporozoite Migration Assay

Sporozoites preincubated ± E-64d (E64) were added to Hepa 1-6 cells, and migratory activity was measured using two different assays. On the left is the calcein assay, in which sporozoites were incubated for 1 hr with Hepa 1-6 cells preloaded with calcein, and the amount of fluorescent calcein released into the medium was measured using a fluorimeter. Fluorescence is expressed as arbitrary units (a.u.). On the right is the dextran assay, in which sporozoites were added to Hepa 1-6 cells in the presence of dextran-FITC, and the number of fluorescent cells per 20 fields is shown. Controls include salivary glands from uninfected mosquitoes (sg) and sporozoites (spz) treated with cytochalasin D (CD). As a control for the effect of E-64d on wound healing, Hepa 1-6 cells ± E-64d were wounded by scratching with a razor blade in the presence of dextran-FITC and allowed to heal for 1 hr, and the number of FITC-positive cells in 100 fields were counted (scratch test). Shown are means ± SD of triplicates.

monolayers, sporozoites move in circles so that sporozoites that migrate for a long time wound a few cells over and over again whereas those that migrate for a short time wound the same few cells but less frequently. This difference in migratory behavior can be measured by determining the extent of release of an intracellular dye such as calcein green-AM. When Hepa 1-6 cells were loaded with calcein green-AM, incubation with freshly isolated sporozoites caused measurable release of the dye, while uninfected salivary gland material had no effect (Figure 1). This result was dependent on sporozoite motility as treatment with cytochalasin D, an inhibitor of motility, caused minimal release of calcein.

We next compared sporozoite migratory activity in the presence or absence of E-64d, a cysteine protease inhibitor that inhibits CSP processing and productive invasion (Coppi et al., 2005). Treatment with E-64d caused a five-fold increase in calcein release, suggesting that when sporozoites are inhibited from productively invading a cell, they continue to migrate (Figure 1). In contrast, the dextran-uptake assay does not distinguish between E-64d treated and untreated sporozoites (Figure 1). Because repeated wounding of a cell may lead to its rupture with release of all intracellular calcein, the calcein assay may not be completely linear, although it would still reflect the sporozoites' overall migratory activity. Importantly, E-64d does not interfere with the resealing of the wound in Hepa 1-6 cells as cells mechanically wounded in the absence or presence of E-64d showed no difference in the number of dextran-positive cells (Figure 1).

Highly Sulfated HSPGs Inhibit Migration and Promote Invasion by Sporozoites

Previous work has shown that sporozoites bind to the glycosaminoglycan chains (GAGs) of HSPGs (reviewed in Sinnis and Coppi, 2007). In addition, the sulfate moieties of GAGs are critical for sporozoite binding and a high over-all density of sulfation is required (Pinzon-Ortiz et al., 2001). To determine whether highly sulfated heparan sulfate might direct sporozoites to stop migrating and actively invade hepatocytes, we treated Hepa 1-6 cells with chlorate, a metabolic inhibitor of sulfation that decreases the extent of GAG sulfation (Humphries and Silbert, 1988), and monitored sporozoite migration. Previous studies in hepatoma cells indicated that treatment with 10 mM and 30 mM chlorate decreased incorporation of $^{35}SO_4$-sulfate into proteoglycans by 60% and 75% respectively, with no effect on protein synthesis or cell growth (Pinzon-Ortiz et al., 2001). When sporozoites were added to cells pretreated with chlorate, their migratory activity increased in a manner dependent on the dose of chlorate (Figure 2A). At 20 mM chlorate, their migratory activity was equivalent to that of parasites treated with E-64d. Importantly, chlorate-treatment had the opposite effect on sporozoite invasion with a dose-dependent inhibition of this process (Figure 2A and Figure S1 in the Supplemental Data available with this article online). The effect was specific to inhibition of sulfation by chlorate, as adding back sulfate to the chlorate-treated cells restored the ability of sporozoites to productively invade (Figure S1). These findings indicate that the sulfation state of HSPGs dramatically changes the nature of the interaction between sporozoites and host cells.

Since reliable markers for the early parasitophorous vacuole (PV) in sporozoite infection are lacking, it is difficult to distinguish invading from migrating sporozoites. To address this issue, we performed invasion assays in the presence of E-64d, which inhibits productive invasion of cells (Coppi et al., 2005) and therefore allows us to approximate the number of intracellular parasites that are in the process of migrating. As shown in Figure 2A, there are few intracellular sporozoites in the presence of E-64d, indicating that the majority of intracellular sporozoites in the absence of E-64d have productively invaded. Chlorate
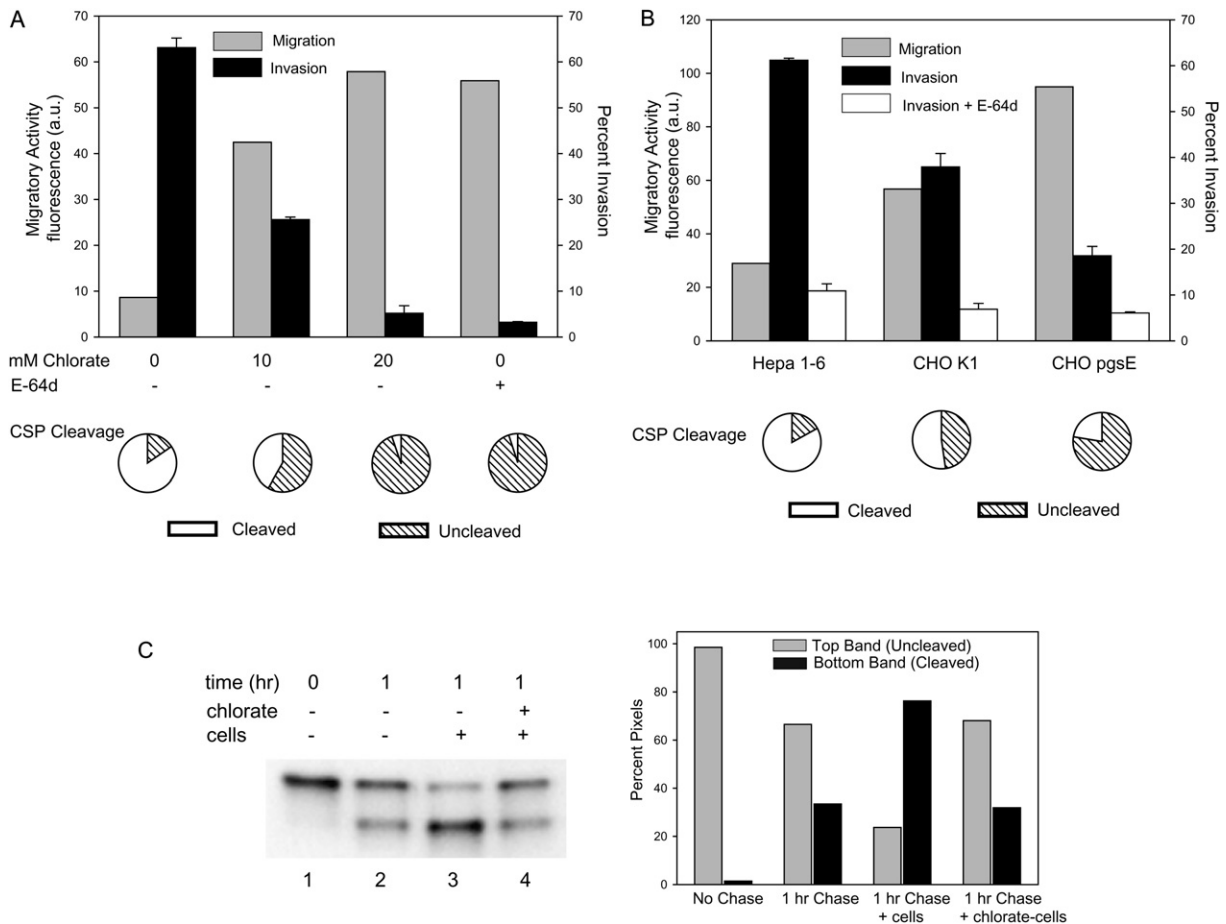
Figure 2. Highly Sulfated HSPGs Arrest Sporozoite Migration and Trigger Invasion and CSP Processing

(A) Effect of chlorate treatment on migration, invasion, and CSP processing. Hepa 1-6 cells were grown in the presence of the indicated amounts of chlorate and washed, and *P. berghei* sporozoites preincubated ±E-64d were added for 1 hr (migration and invasion assays) or 3 min (CSP cleavage assay). To measure migration (gray bars), chlorate-treated Hepa 1-6 cells were preloaded with calcein green, sporozoites were added, and the fluorescence released into the supernatant was measured. Shown are the means of duplicates which did not vary more than ±5%. Invasion (black bars) was quantified by fixing, staining, and counting the numbers of intracellular and extracellular sporozoites. Shown are means ± SD of triplicates. Proteolytic cleavage of CSP (pie charts) was quantified by adding GFP-expressing sporozoites to cells for 3 min and fixing and staining with antiserum specific for full-length CSP. One hundred sporozoites per coverslip were counted, and the pie charts show the percentage of sporozoites with cleaved (white) or full-length (hatched) CSP. Shown are the means of triplicates, which did not vary more than ±5%. All experiments were performed at least three times, and shown are representative experiments.

(B) A CHO cell mutant in HSPG sulfation enhances sporozoite migratory activity and inhibits invasion and CSP cleavage. Sporozoites were incubated with the indicated cell type, and migration (gray bars), invasion in the absence (black bars) or presence (white bars) of E-64d, and CSP cleavage (pie charts) were quantified as described above. For the invasion assay, shown are means ± SD of triplicates. Migratory activity is measured as fluorescence a.u., and shown are the means of duplicates, which did not vary more than ±5%. Pie charts show the means of triplicates, which did not vary more than ±5%. All experiments were performed three times, and shown is a representative experiment.

(C) Quantification of CSP cleavage induced by highly sulfated HSPGs. Sporozoites were metabolically labeled with $^{35}[SO_4]$-Cys/Met and kept on ice (lane 1) or chased for 1 hr (lanes 2–4). They were then spun onto coverslips without cells (lanes 1 and 2) or with cells grown in the absence (lane 3) or presence (lane 4) of chlorate and brought to 37°C for 3 min. Cells and sporozoites were then lysed, and CSP was immunoprecipitated and analyzed by SDS-PAGE and autoradiography. Band intensity was quantified by densitometry and is displayed graphically on the right; gray bars represent uncleaved CSP, and black bars represent cleaved CSP.

had no effect on the percentage of intracellular sporozoites when sporozoites were preincubated with E-64d (Figure S1). These data suggest that sulfation-dependent invasion and the triggering of CSP processing observed when sporozoites contact hepatocytes (Coppi et al., 2005) may share a similar mechanism.

Since chlorate is a general inhibitor of macromolecular sulfation, we also performed experiments with a CHO

cell mutant specifically deficient in sulfation of heparan sulfate (HS) chains. The mutant, CHO pgsE, is derived from the parent cell line CHO K1 and has a mutation in N-deacetylase/N-sulfotransferase (*Ndst1*), which results in the formation of HS with less overall sulfation (Esko et al., 1985). Sporozoite migratory activity was increased in CHO pgsE cells compared to the parental wild-type cell line (Figure 2B). However, sporozoite migration

Table 1. Disaccharide Analysis of Heparan Sulfate on Hepa 1-6 Cells, CHO Cells, Mouse Dermal Fibroblasts, and the Endothelial Cell Line HBMVEC

Sample	Disaccharides (mole %)[a]						
	ΔUA-GlcNAc	ΔUA-GlcNS	ΔUA-GlcNAc6S	ΔUA-GlcNS6S	ΔUA2S-GlcNS	ΔUA2S-GlcNAc6S	ΔUA2S-GlcNS6S
Hepa 1-6	33.21	30.73	10.05	5.52	12.70	0.24	7.55
CHO K1	46.17	13.28	5.52	2.32	22.47	0.00	9.61
CHO pgsE	67.07	14.95	1.20	2.55	6.51	0.00	7.43
MDF	46.08	29.63	10.32	5.67	4.55	0.04	3.70
HBMVEC	69.86	20.08	5.04	2.46	0.78	0.13	1.65

[a] Values are expressed as molar percent and normalized to total protein.

through wild-type CHO cells was increased compared to Hepa 1-6 cells, a difference that is not unexpected, as the HS chains on CHO cells are less sulfated than those found on hepatoma cells (Table 1). Invasion efficiency in these cell lines was inversely correlated to sporozoite migratory activity, with fewer parasites invading the CHO cells with reduced HS sulfation (Figure 2B). Treatment of sporozoites with E-64d, before addition to CHO cells, demonstrated that the majority of intracellular sporozoites had indeed productively invaded (Figure 2B).

Contact with Highly Sulfated HSPGs Induces Proteolytic Cleavage of CSP

Since proteolytic cleavage of the sporozoite's major surface protein, CSP, is associated with productive invasion (Coppi et al., 2005), we next examined whether HSPG sulfation affects CSP cleavage. CSP cleavage was monitored by immunostaining sporozoites with antisera that only recognize uncleaved, full-length CSP. Chlorate treatment reduced CSP cleavage in a dose-dependent manner (Figure 2A, pie charts), and cleavage of surface CSP was also reduced when sporozoites encountered CHO cells containing less sulfated HSPGs (Figure 2B, pie charts). Thus, proteolytic processing of CSP closely paralleled the invasion rate and was inversely correlated to sporozoite migratory activity.

CSP cleavage occurs rapidly upon contact with hepatocytes but is a significantly slower process in the absence of cells (Coppi et al., 2005). To confirm in a more quantitative manner that highly sulfated HSPGs induce CSP cleavage, metabolically labeled sporozoites were chased for 1 hr so that labeled CSP had time to be exported to the sporozoite surface. The labeled sporozoites were then added to either chlorate-treated or untreated Hepa 1-6 cells. As shown, a small amount of labeled CSP was cleaved in the absence of cells during the 1 hr chase (Figure 2C, compare lanes 1 and 2 and see graph). However, when labeled and chased sporozoites were added to Hepa 1-6 cells for 3 min, the majority of labeled CSP was rapidly cleaved (Figure 2C, lane 3 and see graph). This cell-induced cleavage was prevented when Hepa 1-6 cells were pretreated with chlorate (Figure 2C, lane 4 and see graph). Taken together, these results indicate that rapid cleavage of CSP is induced by highly sulfated HS chains found on the hepatocyte surface.

Sporozoites Preferentially Migrate through Dermal Fibroblasts and Endothelial Cells and Do Not Efficiently Invade These Cells

The finding that sulfation of HS chains plays a role in the sporozoite's "decision" to migrate or invade a cell is likely to be relevant in vivo, where the density of HS sulfation differs among organs. HSPGs on hepatocytes are among the most highly sulfated in the mammalian host, and those found on endothelial cells and in the dermis are, in comparison, less sulfated (Lindblom and Fransson, 1990; Lyon et al., 1994). Our data, therefore, suggested that sporozoites use the sulfation density of HSPGs to ascertain where they are and whether they should continue to migrate or prepare for cell invasion.

To test this hypothesis, we studied the interaction of sporozoites with cell types they are likely to encounter on their way to the liver, namely, dermal fibroblasts and endothelial cells. First, we examined the sulfation of HS produced by mouse dermal fibroblasts (MDF) and endothelial cells (HBMVEC) compared to Hepa 1-6 cells and CHO cells (Table 1). The overall extent of sulfation, as measured by summing the amount of N-sulfated glucosamine, 6-O-sulfated glucosamine, and 2-O-sulfated uronic acids, increased from 0.4 sulfate residues/disaccharide in HBMVEC to 0.6, 0.8, and 1 sulfate/disaccharide in MDF, CHO, and Hepa 1-6 cells, respectively (Table 1). Thus, hepatocytes produce HS with a higher content of sulfate compared to other cells a sporozoite may encounter in the mammalian host.

Sporozoite migration experiments in dermal fibroblasts, endothelial cells, and hepatocytes showed that migratory activity correlated inversely with overall sulfation of the cell type encountered (Figure 3A and Table 1). To insure that wounding by sporozoites had the same effect in these different cell lines, we incubated each cell type with maximally migrating, i.e., E-64d-treated sporozoites. Similar amounts of calcein were released by each cell line, indicating that inherent differences among them do not lead to significant differences in the damage caused by migrating sporozoites (Figure S2).

In contrast to the migratory activity of sporozoites in dermal fibroblasts and endothelial cells, productive invasion and CSP processing were decreased in these cells (Figure 3A). In addition, when sporozoites were placed on freshly excised mouse skin they retained full-length
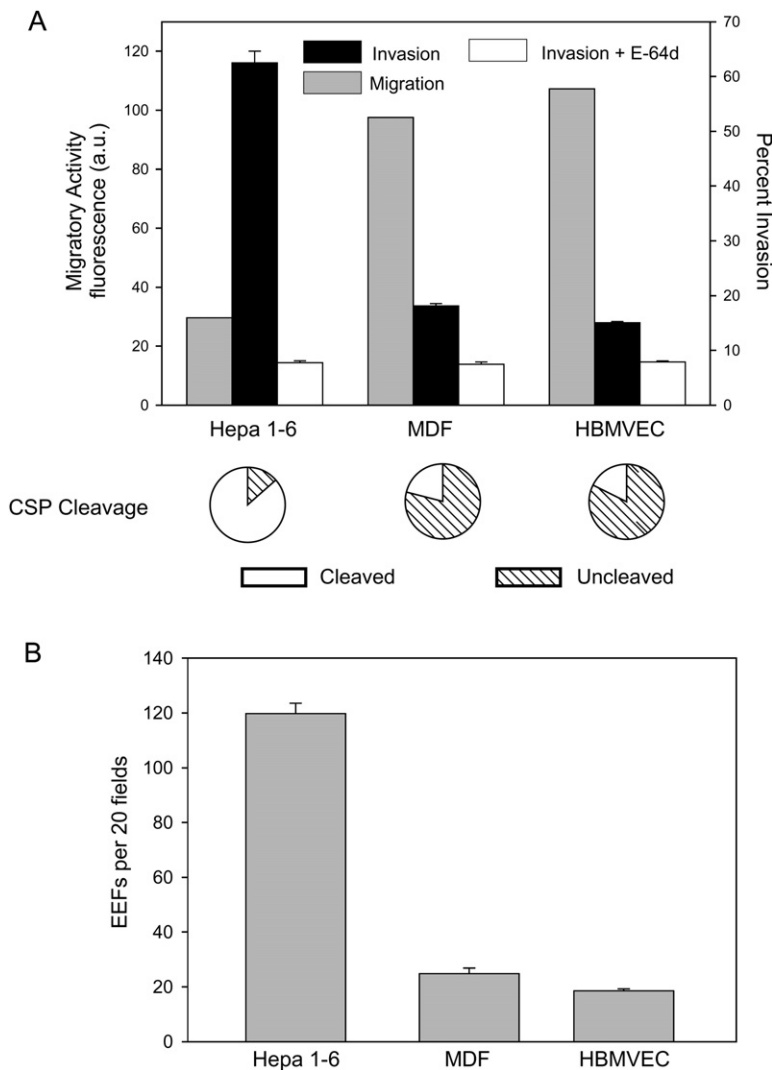
Figure 3. Sporozoite Contact with Endothelial Cells and Dermal Fibroblasts Leads to Increased Migratory Activity and Decreased Productive Invasion and CSP Cleavage

(A) Sporozoites were incubated with Hepa 1-6 cells, dermal fibroblasts (MDF), or an endothelial cell line (HBMVEC), and migration (gray bars), invasion in the absence (black bars) or presence (white bars) of E-64d, and CSP cleavage (pie charts) were quantified as previously described. For the invasion assay, shown are means ± SD of triplicates. Migratory activity is measured as fluorescence a.u., and shown are the means of duplicates, which did not vary more than ±5%. Pie charts show the means of triplicates, which did not vary more than ±5%. All experiments were performed three times, and shown are representative experiments.

(B) Development of EEFs in dermal fibroblasts and endothelial cells. Sporozoites were added to the indicated cell line, and 44 hr later cells were fixed and stained, and EEFs were counted. Shown are means ± SD of triplicates. This experiment was performed three times, and shown is a representative experiment.

CSP on their surface, whereas those placed on liver sections had predominantly cleaved CSP on their surface (Figure S3).

The number of intracellular sporozoites in MDFs and HBMVECs was higher than that observed with E-64d-treated parasites, suggesting that sporozoites can productively invade these cells. Further studies showed that sporozoites could develop in dermal fibroblasts and endothelial cells, albeit at a low efficiency (Figure 3B). Overall, these data suggest that, after their injection into the mammalian host, sporozoites preferentially migrate through those cell types in which they cannot efficiently replicate and are activated, by the high level of HS sulfation, to productively invade hepatocytes.

Soluble Heparin Induces CSP Cleavage and Augments Invasion of Cell Lines with Low Levels of Sulfated HSPGs

To determine whether the effect of highly sulfated HS chains on sporozoites was dependent upon cell contact,

we tested the effect of soluble heparin (a highly sulfated form of heparan sulfate) on CSP cleavage and sporozoite invasion. In the absence of cells, 5 µg/ml of soluble heparin induced CSP cleavage in 40% of sporozoites (Figure 4A). We then tested whether a short preincubation with this concentration of heparin could enhance sporozoite infectivity for cells that have undersulfated HSPGs. Indeed, soluble heparin could partially compensate for the lack of sulfated HSPGs on these cells and enhanced sporozoite infectivity for these normally less permissive cell lines (Figure 4B). Interestingly, the dose-response curve for CSP cleavage had an inverted bell shape. One explanation for this type of dose response is that heparin at low dose allows CSP multimers or CSP/protease complexes to form, which facilitate cleavage and invasion. At high doses of heparin, complexes fail to form due to titration of the individual factors. Activation of growth factor signaling by heparin shows a similar response, which has been interpreted as binding of heparin to both the growth factor and the receptor (Pellegrini, 2001).
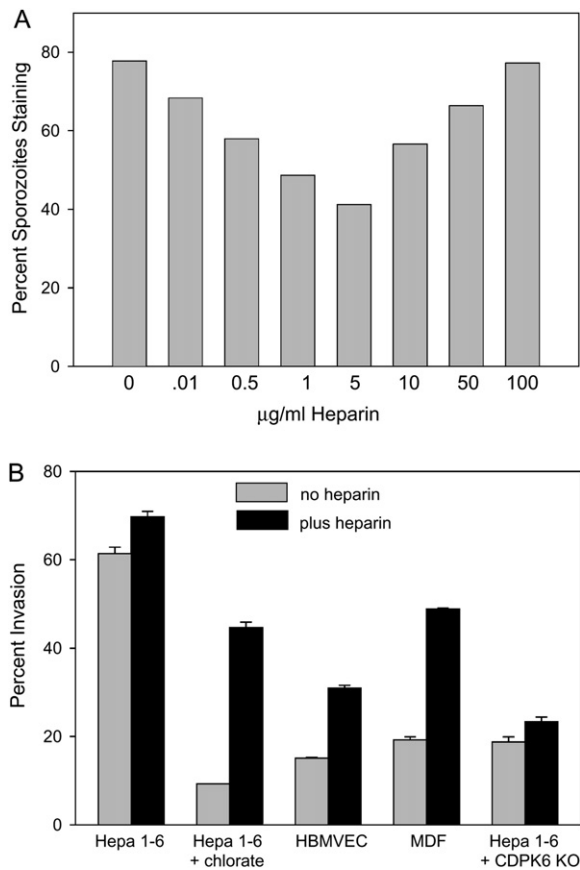
Figure 4. Soluble Heparin Induces CSP Cleavage and Enhances Sporozoite Invasion of Nonpermissive Cells

(A) CSP cleavage after a 5 min incubation with the indicated concentrations of heparin was quantified by fixing and staining sporozoites with antisera specific for full-length CSP. Two hundred sporozoites per well were counted, and shown is the percentage of sporozoites staining. This experiment was repeated three times with identical results.

(B) Sporozoite invasion of the indicated cell line was quantified by adding wild-type or *CDPK-6* mutant (CDPK6 KO, see below) sporozoites preincubated for 5 min with medium alone (gray bars) or medium containing 5 μg/ml heparin (black bars) to Hepa 1-6 cells grown in the absence or presence of chlorate, HBMVEC, or MDF cells. After 1 hr, cells were fixed and stained, and the numbers of intracellular and extracellular sporozoites were counted. Shown are means ± SD of triplicates. This experiment was repeated twice with identical results.

Sporozoite Binding to Heparin Induces a Signaling Cascade

The ability of highly sulfated HSPGs on the host cell surface (and soluble heparin) to trigger CSP cleavage and productive invasion of cells suggests that downstream signaling events occur following the sporozoite's interaction with optimally sulfated HSPGs. Therefore, we tested the effect of staurosporine, a broad-spectrum protein kinase inhibitor, previously shown to inhibit *Plasmodium* invasion but not motility (Mota et al., 2001; Ward et al., 1994), on sporozoite migration, invasion, and CSP cleavage. Pretreatment with staurosporine increased sporozoite migration, while invasion and CSP cleavage were in-

hibited, indicating that a parasite protein kinase was potentially involved in this process (Figure 5).

Although staurosporine is not specific for a particular family of protein kinases, it is slightly more active against kinases of the protein kinase C (PKC) family, which in higher eukaryotes are activated by calcium and play a central role in calcium-mediated signaling. No obvious PKC-like kinases have been found in the *Plasmodium* genome database (Ward et al., 2004); however, *Plasmodium* has a family of calcium-dependent protein kinases (CDPKs; Ward et al., 2004) that function to transduce calcium-mediated signals (Billker et al., 2004; Ishino et al., 2006; Siden-Kiamos et al., 2006). Since calcium signaling plays a central role in the regulation of cell invasion in both *Plasmodium* and the related parasite, *Toxoplasma gondii* (Carruthers and Sibley, 1999; Mota et al., 2002), we hypothesized that, after sporozoite binding to highly sulfated HSPGs, one of the CDPKs may play a role in the sporozoite's transition from a migratory to an invasive phenotype. Selective CDPK inhibitors have not been described, but the calmodulin antagonist W-7 targets the calmodulin-like domain of plant CDPKs, and KN-93 inhibits the structurally related animal calmodulin-dependent protein kinase II. Like staurosporine, these inhibitors enhanced migration but inhibited cell invasion and CSP processing (Figure 5). Purvalanol A, an inhibitor of cyclin-dependent kinases, was used as a control and had no effect on sporozoite migration, invasion, or CSP cleavage. Together, these data suggest that binding of sporozoites to highly sulfated HS chains triggers a signaling cascade involving one of the *Plasmodium* CDPKs.

CDPK-6 Signaling Is Required for the Switch from Migration to Invasion

*CDPK*s in *Plasmodium* are present as a multigene family, and initial mining of the *Plasmodium falciparum* genome database suggested that this family had five members (Ward et al., 2004). With the exception of *CDPK-2*, all of the *CDPK* genes have clear orthologs in the rodent malaria parasite genomes (Hall et al., 2005). Our analysis indicates that a sixth conserved gene, which we call *CDPK-6*, should be grouped within the *CDPK* family. *CDPK-6* is predicted to encode an atypically large protein, characterized by a CDPK-like kinase domain, an incomplete carboxy-terminal calmodulin-like domain, and an unusually large amino-terminal extension. The *P. falciparum* transcriptome shows that transcription of Pf*CDPK-6* (PF11_0239) is significantly upregulated in the sporozoite stage (Le Roch et al., 2003). To determine if this kinase has a role in the switch from migration to invasion, we generated a *CDPK-6* gene knockout by replacing the coding region of *P. berghei CDPK-6* (PB001122.01.0) with a resistance marker via double homologous recombination (Figure 6A). Resistant parasites were selected and cloned, and integration of the targeting construct into the *CDPK-6* locus was verified by pulse-field gel electrophoresis and Southern blot analysis (Figure 6B).

CDPK-6 mutant parasites produced fewer salivary gland sporozoites (R.T., A.C., P.S., and O.B., unpublished
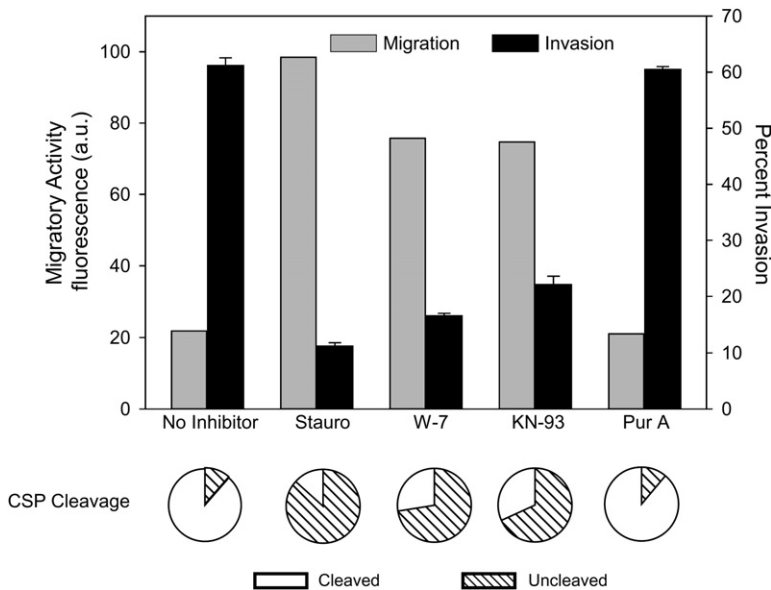
Figure 5. Kinase Inhibitors Enhance Sporozoite Migration, Inhibit Invasion, and Decrease CSP Cleavage

P. berghei sporozoites preincubated with the indicated inhibitors were added to Hepa 1-6 cells for 1 hr (migration and invasion assays) or 3 min (CSP cleavage assay). Migration (gray bars), invasion (black bars), and proteolytic cleavage of CSP (pie charts) were quantified as previously outlined. For the invasion assay, shown are means ± SD of triplicates. Migration is measured as fluorescence a.u., and shown are the means of duplicates, which did not vary more than ±5%. Pie charts show the means of triplicates, which did not vary more than ±5%. All experiments were performed three times, and shown are representative experiments. Stauro, staurosporine; Pur A, purvalanol A.

data); however, we were able to obtain sufficient numbers for the present study. As shown in Figure 6C, *CDPK-6* mutant sporozoites displayed enhanced migratory activity and were significantly less infective for hepatocytes. Importantly, preincubation of *CDPK-6* mutant sporozoites with soluble heparin could not enhance their invasive capacity (Figure 4B), further supporting our hypothesis that CDPK-6 transduces the signal resulting from sporozoite contact with highly sulfated HSPGs. We have confirmed these findings in vivo, where there was significant delay in the time to detectable blood-stage infection with *CDPK-6* mutant sporozoites compared to wild-type (data not shown). In addition, the majority of *CDPK-6* mutant sporozoites did not cleave CSP upon contact with hepatocytes (Figure 6C, pie charts), and pulse-chase metabolic labeling experiments confirmed that they were deficient in their ability to cleave CSP (Figure 6D).

The finding that *CDPK-6* mutant sporozoites can productively invade Hepa 1-6 cells to a small extent (Figure 6C, CDPK-6 KO ± E-64d) suggested that CDPK-6 was not the only kinase involved in the transition to an invasive phenotype. To test this, we performed invasion assays with wild-type and *CDPK-6* mutant sporozoites in the presence of the protein kinase A (PKA) inhibitor H-89, since PKA inhibitors have been shown to affect activation of sporozoites (A. Rodriguez and L. Cabrita-Santos, personal communication). This inhibitor decreased invasion by wild-type sporozoites by approximately 30% and further decreased invasion of the *CDPK-6* mutant sporozoites (Figure 6C). In agreement with this finding, H-89 enhanced migration of wild-type sporozoites and further enhanced the migratory activity of *CDPK-6* mutant sporozoites. Together, these data suggest that CDPK-6 works in concert with other signaling molecules to induce an invasive phenotype. These data were confirmed with a second *CDPK-6* mutant generated by an independent transfection experiment (Figure S4).

DISCUSSION

In this report we show that HSPGs provide an environmental signal that modulates the behavior of *Plasmodium* sporozoites. Using chlorate-treated Hepa 1-6 cells and a CHO cell mutant defective in an enzyme required for HS sulfation, we found that sporozoites preferentially migrate in the presence of HSPGs with low levels of sulfation, whereas contact with cells expressing highly sulfated HSPGs triggers CSP cleavage and productive invasion. These findings are of relevance in the mammalian host, where we found that sporozoites preferentially migrate through dermal fibroblasts and endothelial cells and productively invade hepatocytes. Importantly, the HS chains expressed on the surface of these different cell types parallel the HSPG sulfation level of the organs from which they are derived. These data, therefore, suggest a mechanism by which sporozoites navigate in the mammalian host and retain their infectivity for a cell that is some distance from where they are deposited by infected mosquitoes.

Sporozoites recognize these highly sulfated HS chains, likely via binding of their major surface protein, CSP. Previous studies have shown that CSP has two heparin-binding sites, one in the NH_2 terminus and one in a cell-adhesive motif, the type 1 thrombospondin repeat (TSR), found in the COOH-terminal portion of the protein (Rathore et al., 2002; Sinnis et al., 1994). Our model is that the NH_2-terminal portion of CSP binds to and is cross-linked by highly sulfated HSPGs, resulting in a signaling cascade that is mediated, at least in part, by CDPK-6. Activation of CDPK-6 leads to secretion of the protease that cleaves CSP, thereby exposing the TSR, which binds with high affinity to HSPGs, resulting in productive invasion of the hepatocyte (Figure 7). Thus, this model encompasses glycosaminoglycan-dependent induction of a key signaling response in a pathogen.
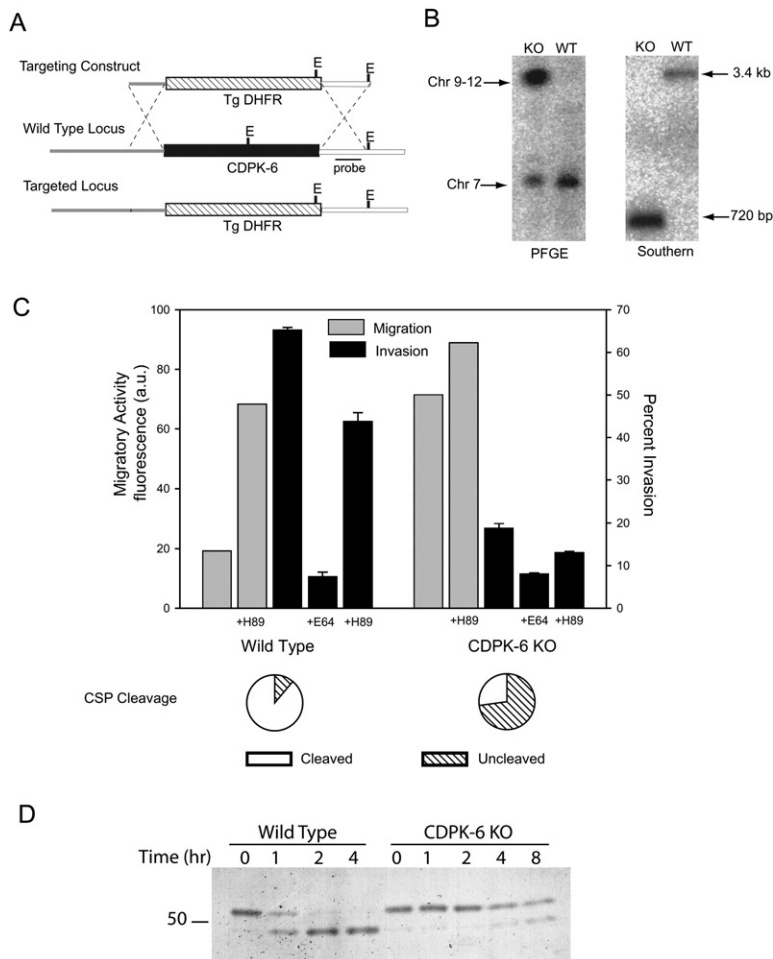
Figure 6. Construction and Phenotypic Characterization of *CDPK-6* Mutant Sporozoites

(A) Strategy used to target the *CDPK-6* locus (black box). The targeting construct contained the selectable marker cassette (*T. gondii DHFR-TS* with upstream and downstream control elements of *P. berghei DHFR-TS*; hatched box) flanked by the 5′UTR of *CDPK-6* (thick gray line) and the 3′UTR of *CDPK-6* (thick white line) to target recombination. EcoRV sites are labeled "E."

(B) Confirmation of genotype. Transfected clones were checked by PFGE using a probe specific for the 3′UTR of *P. berghei DHFR-TS*, which detects the wild-type *DHFR-TS* locus on chromosome 7 and the altered *CDPK-6* locus in the transgenic parasites consistent with its location on chromosome 9. Clones were also checked by Southern blot after digestion of genomic DNA with EcoRV. The probe specific for the 3′UTR of *CDPK-6* (black line in [A]) detects diagnostic fragments of 3.4 kb in wild-type and 725 bp in transgenic parasites.

(C) Wild-type or *CDPK-6* mutant *P. berghei* sporozoites were preincubated in medium alone, the PKA inhibitor H-89, or E-64d as indicated and added to Hepa 1-6 cells, and migration (gray bars), invasion (black bars), or CSP cleavage (pie charts) were measured as previously outlined. For the invasion assay, shown are means ± SD of triplicates. Migration is measured as fluorescence a.u., and shown are the means of duplicates, which did not vary more than ±5%. Pie charts show the means of triplicates, which did not vary more than ±5%. All experiments were performed twice, and shown are representative experiments.

(D) Wild-type or *CDPK-6* mutant *P. berghei* sporozoites were metabolically labeled with $^{35}[SO_4]$-Cys/Met and kept on ice (time 0) or chased for the indicated times. Sporozoites were then lysed, and CSP was immunoprecipitated and analyzed by SDS-PAGE and autoradiography.

Several lines of evidence indicate that, in *Plasmodium*, CDPKs translate calcium signals into a wide variety of stage specific end points. In gametocytes, CDPK-4 transduces the calcium signal in male gametocytes that leads to exflagellation (Billker et al., 2004). In ookinetes, mobilization of intracellular calcium and transduction of this signal through CDPK-3 enables the ookinete to glide and penetrate the mosquito midgut wall (Ishino et al., 2006; Siden-Kiamos et al., 2006). Previous studies have shown that calcium is an important second messenger regulating invasion of *Plasmodium* sporozoites and *Toxoplasma* tachyzoites (Mota et al., 2002; Carruthers and Sibley, 1999), and here we show that this signal is, in part, transduced by CDPK-6. Together, these studies suggest that *Plasmodium* CDPKs are a family of protein kinases that translate the ubiquitous second messenger calcium into different stage-specific cellular responses.

The function of cell traversal by sporozoites has been the subject of much debate. Although this study does not directly address the role of migration, our finding that a sporozoite's migratory activity is inversely correlated to how efficiently it invades a particular cell line demonstrates that migration per se is not sufficient to promote productive invasion. A previous study has suggested that cell traversal activates sporozoites for productive infection via a hepatocyte cytosolic factor (Mota et al., 2002). However, our data demonstrate that sporozoite activation is primarily due to contact with highly sulfated HSPGs on the cell surface and can, at least in part, be induced with soluble heparin in a cell-free system. Nonetheless, our data as well as that of others, indicate that a small amount of migration takes place within hepatocytes (Figures 2, 3, and 5 and Mota et al., 2002), suggesting that sporozoite activation is a progressive process that is initiated by contact with highly sulfated HSPGs. Continued migration through hepatocytes, therefore, may lead to exposure of additional adhesins that are required for productive invasion. The idea that activation is a progressive
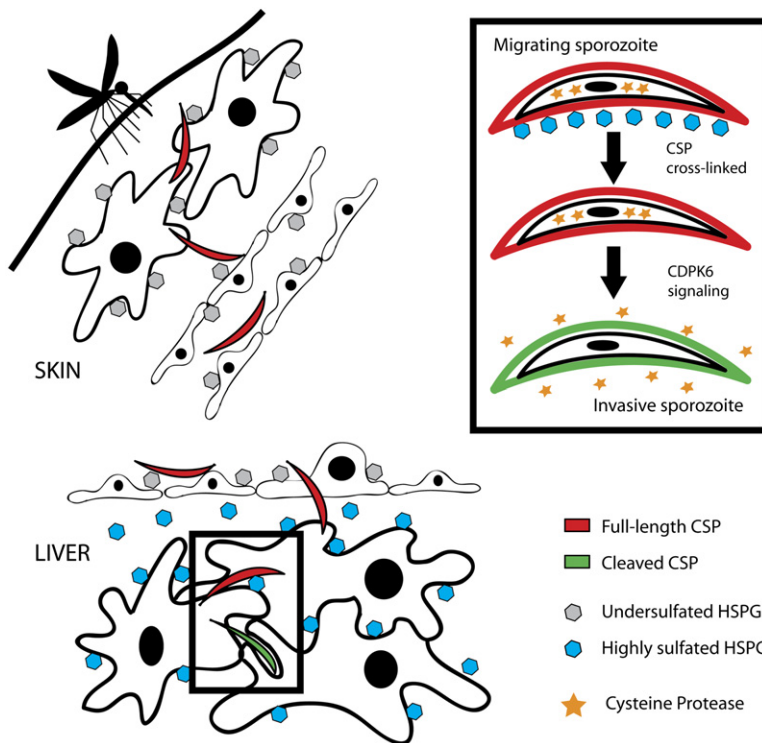
Figure 7. Model of Sporozoite Activation for Invasion by Highly Sulfated HSPGs
Migratory sporozoites (red) are injected into the dermis by an infected mosquito, where they encounter cells expressing undersulfated HSPGs (gray hexagons). They traverse endothelial cells, also expressing undersulfated HSPGs, and enter the bloodstream. In the liver they cross the sinusoidal barrier and encounter the highly sulfated HSPGs found in the loose basement membrane of the liver (space of Disse) and on hepatocytes (blue hexagons) and become activated for productive invasion (green sporozoites). The inset shows some of the specific steps involved in sporozoite activation, namely crosslinking of CSP by highly sulfated HSPGs, which results in a CDPK-6-dependent signaling pathway associated with the secretion of a parasite cysteine protease (stars) that proteolytically processes surface CSP.

process is consistent with previous data suggesting that highly sulfated HSPGs of hepatocytes protrude through the open fenestrations of the liver sinusoids and arrest circulating sporozoites (reviewed in Sinnis and Coppi, 2007). The sporozoite's switch to ''invasion mode'' may therefore begin in the liver sinusoid and progress as the sporozoite crosses this barrier and enters the liver parenchyma.

The switch to ''invasion mode'' is no doubt accompanied by a multitude of events, many of which have not yet been elucidated. Recently, the secretion of two proteins with 6-cys motifs, Pbs36p and Pbs36, has been associated with productive invasion (Ishino et al., 2005). However, whether they play a role in initiating invasion or at some later point is not yet known (van Dijk et al., 2005). In this study we found that proteolytic cleavage of CSP is an early event in this process. Although the responsible protease is not yet known, our data suggest that the switch to invasion mode results in either secretion of the protease onto the sporozoite surface or activation of a protease that may already be present on the parasite surface. Nonetheless, our findings elucidate both the host cell molecule initiating proteolytic processing of a *Plasmodium* adhesin and the kinase that transduces this signal, perhaps providing a model for adhesin-specific processing in other *Plasmodium* life-cycle stages and other Apicomplexa. Further studies to determine additional events that occur upon CDPK-6 signaling in response to contact with highly sulfated HSPGs are ongoing.

In conclusion, our data suggest that migration through cells is the default behavior of the newly injected sporozoite and that this behavior is maintained as long as the sporozoite encounters cells expressing HSPGs with low levels of sulfation. Once in the liver, where the HSPGs are highly sulfated, the sporozoite undergoes activation via a calcium-dependent kinase, resulting in controlled proteolysis of surface CSP and a shift to invasion mode to begin the next stage of malaria infection (Figure 7). These findings begin to unravel how *Plasmodium* sporozoites optimize their infectivity for an organ that is a significant distance from the skin, where their journey begins.

EXPERIMENTAL PROCEDURES

Parasites
Three- to five-day-old *Anopheles stephensi* mosquitoes were fed on Swiss Webster mice infected with either *P. berghei* (ANKA or NK65 strain), GFP-transgenic *P. berghei* (Janse et al., 2006), or the *CDPK-6* mutant. For experiments with *CDPK-6* mutant parasites, controls were the ANKA strain. On days 18 to 20, post-infective blood meal, mosquitoes were anesthetized on ice, rinsed in 70% ethanol, and washed in Dulbecco's modified Eagle's medium (DMEM), and the salivary glands were removed. Tissue was gently ground in a tissue homogenizer and centrifuged at 80 × g for 3 min to remove mosquito debris, and sporozoites were counted in a hemocytometer.

Antibodies
mAb 3D11 is directed against the repeat region of *P. berghei* CSP and, for some experiments, was conjugated to sepharose as described (Coppi et al., 2005). Polyclonal antisera to the NH$_2$-terminal third of CSP was generated in rabbits as previously described and is used to detect full-length CSP (Coppi et al., 2005).

Cells
All cells were maintained in DMEM supplemented with 10% fetal calf serum and 1 mM glutamine (DMEM/FCS), except CHO cells, which were grown in Ham's F-12 medium supplemented with 7.5% FCS, and HBMVEC cells, which were grown in EGM-2MV media (Cambrex,

Rockland, ME) supplemented with 5% FCS. CHO cell mutant pgsE defective in GlcNAc N-deacetylase/N-sulfotransferase 1 (*Ndst1*) was derived from wild-type CHO K1 cells and was described previously (Bame and Esko, 1989). Other cell lines were obtained from the following sources: Hepa 1-6 cells (CRL −1830; ATCC, Rockville, MD); HBMVEC, a human endothelial cell line (CC-2811; Cambrex); mouse dermal fibroblasts were isolated from Balb/C mice as previously described (Freshney, 2000 and Supplemental Data).

Chlorate Treatment of Cells
Hepa 1-6 cells were seeded on glass coverslips (2.5×10^5/well) and grown overnight in low-sulfate medium (Ham's F-12, 1 mM glutamine, and 2% FCS that had been dialyzed extensively versus 150 mM NaCl, 10 mM HEPES [pH 7.3]) with the indicated concentration of sodium chlorate. An appropriate amount of medium was replaced with water to maintain normal osmolarity. On the following day, cells were washed twice with DMEM not containing chlorate, and sporozoites were added in DMEM/FCS.

Metabolic Labeling
P. berghei sporozoites were metabolically labeled in DMEM with [^{35}S]Cys/Met for 1 hr at 28°C, washed, resuspended in DMEM containing 100 μg/ml cycloheximide (to prevent further protein synthesis), and kept on ice or chased. In experiments without host cells, sporozoites were chased for the indicated time at 28°C, and CSP was immunoprecipitated as outlined below. In experiments with host cells, sporozoites were chased for 1 hr at 28°C then centrifuged (300 × g for 5 min at 4°C) onto glass coverslips containing no cells or Hepa 1-6 cells that had been grown in the absence or presence of 20 mM chlorate. Coverslips were incubated at 37°C for 3 min; cells were lysed in 1% Triton X-100, 150 mM NaCl, 50 mM Tris-HCl (pH 8.0) with protease inhibitor cocktail for 1 hr at 4°C; and lysates were incubated with mAb 3D11-Sepharose overnight at 4°C. CSP was eluted with 1% SDS in 0.1 M glycine (pH 1.8), neutralized with 1.5 M Tris-HCl (pH 8.8), and run on a 7.5% SDS-PAGE gel under nonreducing conditions. The gel was fixed, enhanced, dried, and exposed to film. Band intensities were analyzed using a GE Healthcare ImageQuant ECL system with IQuant Capture ECL software.

Cell Contact and CSP Cleavage
P. berghei-GFP sporozoites were centrifuged onto coverslips containing untreated or chlorate-treated cells as outlined above and then incubated at 37°C for 3 min, fixed with 4% paraformaldehyde (PFA), and stained with polyclonal antiserum that recognizes full-length CSP. For experiments using kinase inhibitors, sporozoites were preincubated with 1 μM staurosporine, 50 μM W-7, 100 μM KN-93, or 50 μM purvalanol A for 10 min at 28°C in DMEM; diluted 15-fold with DMEM; and then added to cell monolayers. Sporozoites preincubated with 10 μM E-64d for 15 min at 28°C were used as controls. All inhibitors were obtained from EMD Biosciences (San Diego, CA). In experiments with *CDPK-6* mutant sporozoites, the total number of sporozoites was determined using mAb 3D11, which stains all sporozoites, and the fraction of those staining with antiserum specific for full-length CSP was determined.

Invasion and Development Assays
P. berghei sporozoites (5×10^5) were added to untreated or chlorate-treated cells. When kinase inhibitors were used, sporozoites were preincubated with the inhibitors at the concentrations outlined above for 10 min at 28°C in DMEM, diluted 15-fold with the appropriate culture medium, and added to cells. Sporozoites preincubated with E-64d for 15 min at 28°C were used as controls. For experiments in which it was investigated whether preincubation with heparin could enhance invasion, sporozoites were incubated with 5 μg/ml heparin (Type I-A from porcine intestinal mucosa; Sigma) for 5 min at 28°C in DMEM, diluted 15-fold with DMEM/FCS, and added to cells. After 1 hr at 37°C, cells were washed and fixed, and sporozoites were stained with a double-staining assay that distinguishes intracellular from extracellular

sporozoites as previously outlined (Coppi et al., 2005). For experiments in which development into EEFs was tested, sporozoites were added to the indicated cell line, and after 2 days, cells were fixed and stained, and EEFs were counted.

Dextran Migration Assay
Sporozoites (2×10^4) in DMEM with 0.2% BSA were added to monolayers of Hepa 1-6 cells in the presence of 1 mg/ml FITC-dextran (10,000 MW; Molecular Probes) for 1 hr at 37°C. Cells were washed with DMEM and fixed with 4% PFA, and the number of FITC-positive cells in 100 fields was counted. In some cases, sporozoites were preincubated with 10 μM E-64d or 1 μM cytochalasin D (CD) for 10 min at 28°C and added to cells in the continued presence of E-64d or CD. As a control for the effect of E-64d on wound healing, monolayers of Hepa 1-6 cells were preincubated ±10 μM E-64d for 15 min at 37°C. Following this, 1 mg/ml FITC-dextran was added to the cells, which were then wounded by scratching the coverslip five times with a single-edge razor blade. After 1 hr at 37°C in the continued presence of E-64d, cells were washed and fixed with 4% PFA, and the number of FITC-positive cells in 100 fields was counted.

Calcein Migration Assay
2.5×10^5 cells/well were seeded in 96-well tissue culture-treated plates in medium ± 20 mM chlorate and allowed to grow overnight until semiconfluent. On the day of the experiment, cells were washed with DMEM without phenol red and incubated in this medium with 10 μM calcein green-AM (Molecular Probes) for 1 hr at 37°C, then washed three times. Between 5×10^5 and 1×10^6 sporozoites in culture medium were centrifuged (300 × g at 14°C) onto the calcein-loaded cells and incubated for 1 hr at 37°C. Supernatants containing the released calcein were transferred to a ThermoElectron Microfluor 96-well plate, and fluorescence was read in a Labsystems Fluoroscan II using excitation and emission wavelengths of 485 nm and 538 nm, respectively. For experiments using staurosporine, W-7, KN-93, H-89, or purvalanol A, sporozoites were preincubated in the concentrations used above for 10 min at 28°C in DMEM and diluted 15-fold with the appropriate culture medium before being added to the calcein-loaded cells. Controls included addition of the same number of homogenized uninfected salivary glands and sporozoites preincubated with 10 μM E-64d or 1 μM CD for 10 min at 28°C and added to cells in the continued presence of these inhibitors. Unlike the dextran assay, which is a visual assay and therefore enables few events to be scored, the calcein assay requires larger numbers of sporozoites for signal detection.

Heparin and CSP Cleavage
Sporozoites were incubated in DMEM containing 0–100 μg/ml heparin for 5 min at 28°C, washed twice, fixed with 4% PFA, blocked with 1% BSA/PBS, and stained with polyclonal antiserum that recognizes full-length CSP followed by anti-rabbit Ig conjugated to FITC. One hundred to two hundred sporozoites were counted using phase and fluorescence microscopy, and the percentage of total sporozoites staining for full-length CSP was determined.

Disaccharide Analysis
Confluent cultures of each cell line were washed three times with PBS and lysed with 0.1 N NaOH for 15 min. An aliquot was removed for protein analysis, and the remaining lysate was neutralized with 10 N acetic acid and stored at −20°C until the analysis was performed. HS was isolated from 10^6 cells and purified as described for its isolation from tissues (Grobe et al., 2005; for details see Supplemental Data). HS composition was determined by disaccharide analysis (for details see Supplemental Data), and molar percentages were calculated based on the relative area under each peak. These results were confirmed by a recently developed mass spectrometry-based technique (R.L., R. Cummings, and J.D.E., unpublished data). Results are presented as total disaccharides containing a particular modification.

Construction of *CDPK-6* Mutant Parasites

CDPK-6 mutant *P. berghei* (ANKA) parasites were generated by double homologous recombination using the targeting vector pBS DHFR, in which the *T. gondii* dihydrofolate reductase/thymidilate synthase gene (*DHFR/TS*) is flanked by the upstream and downstream control elements from *P. berghei DHFR/TS*. This cassette confers resistance to pyrimethamine and was targeted to the *CDPK-6* locus (PB001122.01.0) using *CDPK-6* 5′ and 3′UTR sequences (for details see Supplemental Data). A second mutant parasite was made using the same region of homology except that the targeting construct was generated using a two-step PCR method as described in Ecker et al. (2006) (for details see Supplemental Data). Transgenic parasites were generated using the Amaxa Nucleofector (program U33) and 5 μg of DNA as previously outlined (Janse et al., 2006). Selection and cloning by limiting dilution for the generation of *CDPK-6* mutant clones in which the selection cassette replaced the *CDPK-6* coding sequence were carried out as previously described (Janse et al., 2006).

Genotypic Analysis of *CDPK-6* Mutant Parasites

Cloned parasites were genotyped by pulse-field gel electrophoresis (PFGE) and Southern blot analysis. For PFGE, chromosomes were separated on an LKB 2015 Pulsaphor system using a linear ramp of 60–500 s for 72 hr at 4V/cm. The gel was blotted and hybridized with a probe that binds to the 3′UTR of *DHFR/TS*, which detects both the wild-type *DHFR/TS* locus on chromosome 7 and, in the case of the *CDPK-6* mutant, the locus at which the transfected DNA integrated on chromosome 9. For Southern analysis, wild-type and genomic DNA from mutant parasites was digested with EcoRV, and the fragments were separated on a 0.8% agarose gel, blotted onto nylon membrane, and probed with a fragment of *CDPK-6* 3′UTR.

Supplemental Data

The Supplemental Data include Supplemental Experimental Procedures and four supplemental figures and can be found with this article online at http://www.cellhostandmicrobe.com/cgi/content/full/2/5/316/DC1/.

REFERENCES

Amino, R., Thiberge, S., Martin, B., Celli, S., Shorte, S., Frischknecht, F., and Menard, R. (2006). Quantitative imaging of *Plasmodium* transmission from mosquito to mammal. Nat. Med. *12*, 220–224.

Bame, K.J., and Esko, J.D. (1989). Undersulfated heparan sulfate in a Chinese Hamster Ovary cell mutant defective in heparan sulfate N-sulfotransferase. J. Biol. Chem. *264*, 8059–8065.

Bhanot, P., Schauer, K., Coppens, I., and Nussenzweig, V. (2005). A surface phospholipase is involved in the migration of *Plasmodium* sporozoites through cells. J. Biol. Chem. *280*, 6752–6760.

Billker, O., Dechamps, S., Tewari, R., Wenig, G., Franke-Fayard, B., and Brinkmann, V. (2004). Calcium and a calcium-dependent protein kinase regulate gamete formation and mosquito transmission in a malaria parasite. Cell *117*, 503–514.

Carruthers, V.B., and Sibley, L.D. (1999). Mobilization of intracellular calcium stimulates microneme discharge in *Toxoplasma gondii*. Mol. Microbiol. *31*, 421–428.

Coppi, A., Pinzon-Ortiz, C., Hutter, C., and Sinnis, P. (2005). Proteolytic processing of the *Plasmodium* circumsporozoite protein is required for cell invasion. J. Exp. Med. *201*, 27–33.

Ecker, A., Moon, R., Sinden, R.E., and Billker, O. (2006). Generation of gene targeting constructs for *Plasmodium berghei* by a PCR-based method amenable to high throughput applications. Mol. Biochem. Parasitol. *145*, 265–268.

Esko, J.D., Stewart, T.E., and Taylor, W.H. (1985). Animal cell mutants defective in glycosaminoglycan biosynthesis. Proc. Natl. Acad. Sci. USA *82*, 3197–3201.

Freshney, R. (2000). Primary culture. In Culture of Animal Cells: A Manual of Basic Techniques, R. Freshney, ed. (Chichester, NY: Wiley), pp. 149–175.

Grobe, K., Inatani, M., Pallerla, S.R., Castagnola, J., Yamaguchi, Y., and Esko, J.D. (2005). Cerebral hypoplasia and craniofacial defects in mice lacking heparan sulfate Ndst1 gene function. Development *132*, 3777–3786.

Hall, N., Karras, M., Raine, J.D., Carlton, J.M., Kooij, T.W., Berriman, M., Florens, L., Janssen, C.S., Pain, A., Christophides, G.K., et al. (2005). A comprehensive survey of the *Plasmodium* life cycle by genomic, transcriptomic, and proteomic analyses. Science *307*, 82–86.

Humphries, D.E., and Silbert, J.E. (1988). Chlorate: A reversible inhibitor of proteoglycan sulfation. Biochem. Biophys. Res. Commun. *154*, 365–371.

Ishino, T., Yano, K., Chinzei, Y., and Yuda, M. (2004). Cell-passage activity is required for the malarial parasite to cross the liver sinusoidal cell layer. PLoS Biol. *2*, 77–84.

Ishino, T., Chinzei, Y., and Yuda, M. (2005). Two proteins with 6-cys motifs are required for malarial parasites to commit to infection of the hepatocyte. Mol. Microbiol. *58*, 1264–1275.

Ishino, T., Orito, Y., Chinzei, Y., and Yuda, M. (2006). A calcium-dependent protein kinase regulates *Plasmodium* ookinete access to the midgut epithelial cell. Mol. Microbiol. *59*, 1175–1184.

Janse, C.J., Franke-Fayard, B., Mair, G.R., Ramesar, J., Thiel, C., Engelmann, S., Matuschewski, K., van Gemert, G.J., Sauerwein, R.W., and Waters, A.P. (2006). High efficiency transfection of *Plasmodium berghei* facilitates novel selection procedures. Mol. Biochem. Parasitol. *145*, 60–70.

Le Roch, K.G., Zhou, Y., Blair, P.L., Grainger, M., Moch, J.K., Haynes, J.D., De la Vega, P., Holder, A.A., Batalov, S., Carucci, D.J., and Winzeler, E.A. (2003). Discovery of gene function by expression profiling of the malaria parasite life cycle. Science *301*, 1503–1508.

Lindblom, A., and Fransson, L.A. (1990). Endothelial heparan sulphate: Compositional analysis and comparison of chains from different proteoglycan populations. Glycoconj. J. *7*, 545–562.

Lyon, M., Deakin, J.A., and Gallagher, J.T. (1994). Liver heparan sulfate structure. J. Biol. Chem. *269*, 11208–11215.

Mota, M., Pradel, G., Vanderberg, J.P., Hafalla, J.C.R., Frevert, U., Nussenzweig, R.S., Nussenzweig, V., and Rodriguez, A. (2001). Migration of *Plasmodium* sporozoites through cells before infection. Science *291*, 141–144.

Mota, M.M., Hafalla, J.C.R., and Rodriguez, A. (2002). Migration through host cells activates *Plasmodium* sporozoites for infection. Nat. Med. *8*, 1318–1322.

Pellegrini, L. (2001). Role of heparan sulfate in fibroblast growth factor signalling: A structural view. Curr. Opin. Struct. Biol. *11*, 629–634.

Pinzon-Ortiz, C., Friedman, J., Esko, J., and Sinnis, P. (2001). The binding of the circumsporozoite protein to cell surface heparan sulfate proteoglycans is required for *Plasmodium* sporozoite attachment to cells. J. Biol. Chem. *276*, 26784–26791.

Rathore, D., Sacci, J.B., de la Vega, P., and McCutchan, T.F. (2002). Binding and invasion of liver cells by *Plasmodium falciparum* sporozoites. Essential involvement of the amino terminus of circumsporozoite protein. J. Biol. Chem. *277*, 7092–7098.

Siden-Kiamos, I., Ecker, A., Nyback, S., Louis, C., Sinden, R.E., and Billker, O. (2006). *Plasmodium berghei* calcium-dependent protein kinase 3 is required for ookinete gliding motility and mosquito midgut invasion. Mol. Microbiol. *60*, 1355–1363.

Sinnis, P., and Coppi, A. (2007). A long and winding road: The *Plasmodium* sporozoite's journey in the mammalian host. Parasitol. Int. *56*, 171–178.

Sinnis, P., Clavijo, P., Fenyo, D., Chait, B., Cerami, C., and Nussenzweig, V. (1994). Structural and functional properties of region II-plus of the malaria circumsporozoite protein. J. Exp. Med. *180*, 297–306.

van Dijk, M.R., Douradinha, B., Franke-Fayard, B., Heussler, V., van Dooren, M.W., van Schaijk, B., van Gemert, G.J., Sauerwein, R.W., Mota, M.M., Waters, A.P., and Janse, C.J. (2005). Genetically attenuated, P36p-deficient malarial sporozoites induce protective immunity and apoptosis of infected liver cells. Proc. Natl. Acad. Sci. USA *102*, 12194–12199.

Ward, G., Fujioka, H., Aikawa, M., and Miller, L. (1994). Staurosporine inhibits invasion of erythrocytes by malarial merozoites. Exp. Parasitol. *79*, 480–487.

Ward, P., Equinet, L., Packer, J., and Doerig, C. (2004). Protein kinases of the human malaria parasite *Plasmodium falciparum*: The kinome of a divergent eukaryote. BMC Genomics *5*, 79.